MAXILLARY SINUS AUGMENTATION USING AN ENGINEERED POROUS HYDROXYAPATITE: A CLINICAL, HISTOLOGICAL, AND TRANSMISSION ELECTRON MICROSCOPY STUDY IN MAN

Carlo Mangano, MD, DDS
Antonio Scarano, DDS, MD
Giovanna Iezzi, DDS, PhD
Giovanna Orsini, DDS, PhD
Vittoria Perrotti, DDS
Francesco Mangano, DDS
Sergio Montini, DDS
Marcello Piccirilli, BSc
Adriano Piattelli, MD, DDS

KEY WORDS

Biomaterials
Bone engineering
Porous hydroxyapatite
Sinus augmentation procedures

Carlo Mangano, MD, DDS, Francesco Mangano, DDS, *and* ***Sergio Montini, DDS,*** *are in private practice in Gravedona (COMO), Italy.*

Antonio Scarano, DDS, MD, *is a researcher,* ***Giovanna Iezzi, DDS, PhD,*** *is a student and research fellow, and* ***Vittoria Perrotti, DDS,*** *is a research fellow at the Dental School, University of Chieti-Pescara, Chieti, Italy.*

Giovanna Orsini, DDS, PhD, *is a student and research fellow at the Dental School, University of Chieti-Pescara, Chieti, Italy.*

Marcello Piccirilli, BSc, *is a technician with the Dental School, University of Chieti-Pescara, Chieti, Italy.*

Adriano Piattelli, MD, DDS, *is a professor of Oral Pathology and Medicine, Dental School, University of Chieti-Pescara, Via F. Sciucchi 63, 66100 Chieti, Italy (e-mail: apiattelli@unich.it). Address correspondence to Dr Piattelli.*

Porous hydroxyapatite (HA) is a calcium-phosphate–based material that is biocompatible, nonimmunological, and osteoconductive, and has a macroporosity of about 200 to 800 μm. The pores seem to be able to induce migration, adhesion, and proliferation of osteoblasts inside the pore network and to promote angiogenesis inside the pore system. The aim of this study was to evaluate the clinical behavior and the histological and ultrastructural aspects of porous HA in maxillary sinus augmentation procedures. Twenty-four patients (19 men, 5 women; average age 53.4 years) in good general physical and mental health and with partially or completely edentulous maxillae were selected for this study. Six months after sinus floor elevation, at the time of dental implant placement, biopsies were carried out under local anesthesia. These bone cores were cut in half and were processed for light and transmission electron microscopy. After a mean 3 years after implantation, all implants are clinically in function and no surgical or prosthetic complications have occurred. Under light microscopy, newly formed bone was 38.5% ± 4.5%, whereas the residual biomaterial represented 12% ± 2.3% and the marrow spaces represented 44.6% ± 4.2%. In addition, in the majority of cases, the biomaterial particles were in close contact with the bone, which appeared compact with the characteristic features of well-organized lamellar bone. A cement-like line was slightly visible at the bone-biomaterial interface, but there were no gaps or interposed connective tissue in between. A high quantity (about 40%) of newly formed bone was present. Bone was closely apposed to the biomaterials particles as shown in light microscopy and transmission electron microscopy. Moreover, no signs of inflammatory cell infiltrate or foreign body reaction were present. Also, most of the biomaterial was resorbed and only a small quantity (a little more than 10%) was still present. The results of our study show that porous HA can be a suitable synthetic material for bone regeneration in maxillary sinus augmentation procedures.

Introduction

Fresh autologous bone is still considered to be the best grafting material in bone reconstructive surgery, but it has limits, such as poor availability and the necessity of harvesting bone chips from other skeletal sites (intraorally or from the iliac crest). Therefore, additional surgical procedures are needed. Morbidity at donor site is often a problem,[1] particularly when it is necessary to harvest a large amount of bone chips. On the other hand, autologous bone shows resorption patterns proportional to the quantity of harvested material,[2] and this results in a significant loss of grafted bone in large defect fillings. Allogenic bone, however, is available in bone tissue banks, but the serious risk of transmission of viral infections (eg, human immunodeficiency virus, hepatitis, and prions)[3–5] and immunological response restricts the possibilities of a wide use of this material. Synthetic materials avoid these types of risks. They are available in unlimited amounts in various sizes and shapes and can be modified so that they can act as matrix carriers for the delivery of drugs, hormones, growth factors, and stem cells. Among these synthetic materials, porous hydroxyapatite (HA) has been widely studied by several authors.[6–8] Porous HA is a calcium-phosphate–based material and has been studied and used in medicine and dentistry for more than 20 years in specific applications such as dental implants, periodontal defect fillings, alveolar ridge augmentation procedures, and oromaxillofacial surgery.[9–11] Porous HA is approved by the Food and Drug Administration for use in bone surgery and is considered biocompatible, nonimmunological, osteoconductive (ie, it acts as a scaffold for the in-growth of vessels from neighboring bone), and even osteoinductive in some configurations (ie, it can induce pluripotential mesenchymal cells differentiation into functional osteoblasts).[9–15] Macroporosity of porous HA is determined by the presence of pores with a controlled size of about 200 to 800 μm, communicating with each other through micropore interconnections (bimodal porosity, macro- and microporosity). It is demonstrated that pores between 200 and 400 μm are capable of inducing migration, adhesion, and prolifera-

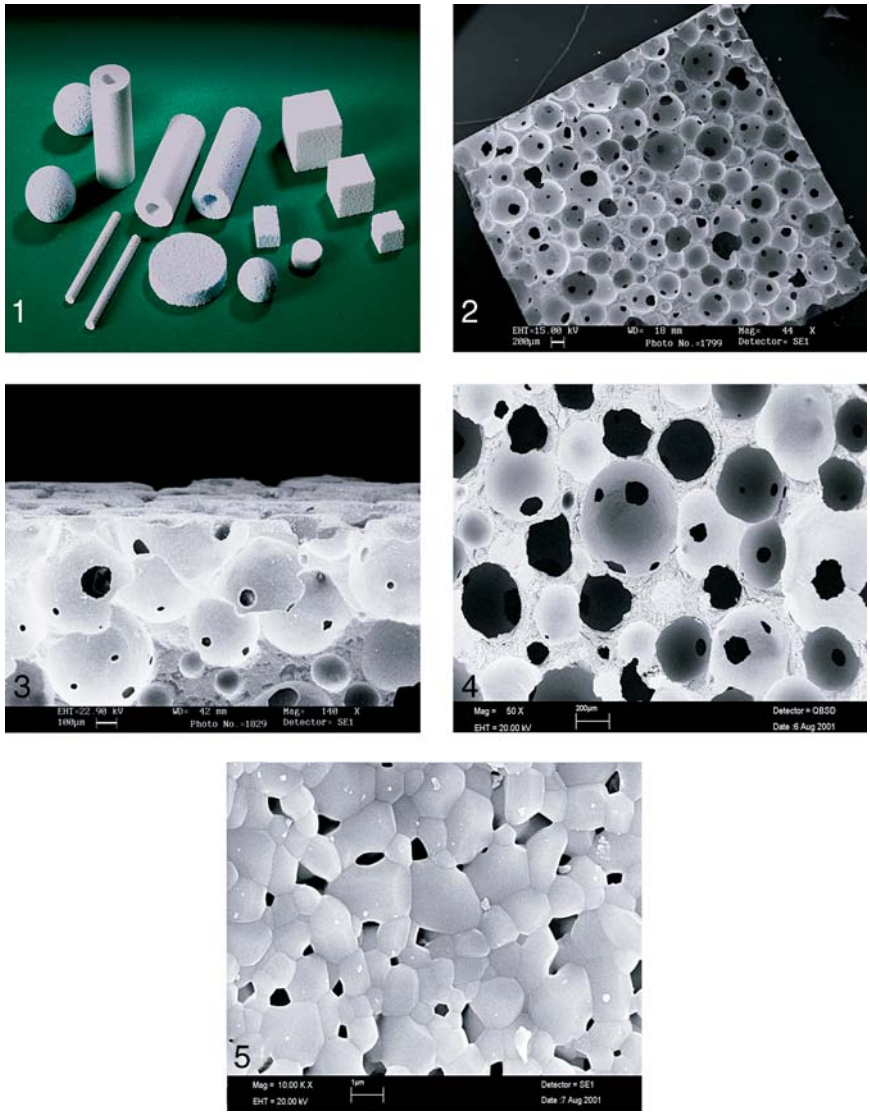

Figures 1–5. Figure 1. Biomimetic biomaterials of porous hydroxyapatite (HA) of different shapes. Figure 2. Macropores of the biomimetic biomaterial and concavities on the surface (original magnification ×44). Figure 3. Another view of HA cube at high magnification (original magnification ×140). Figure 4. Macropore and micropore architecture; note the micropore interconnections within the concavities (original magnification ×50). Figure 5. High magnification showing micropore interconnections (original magnification ×1000).

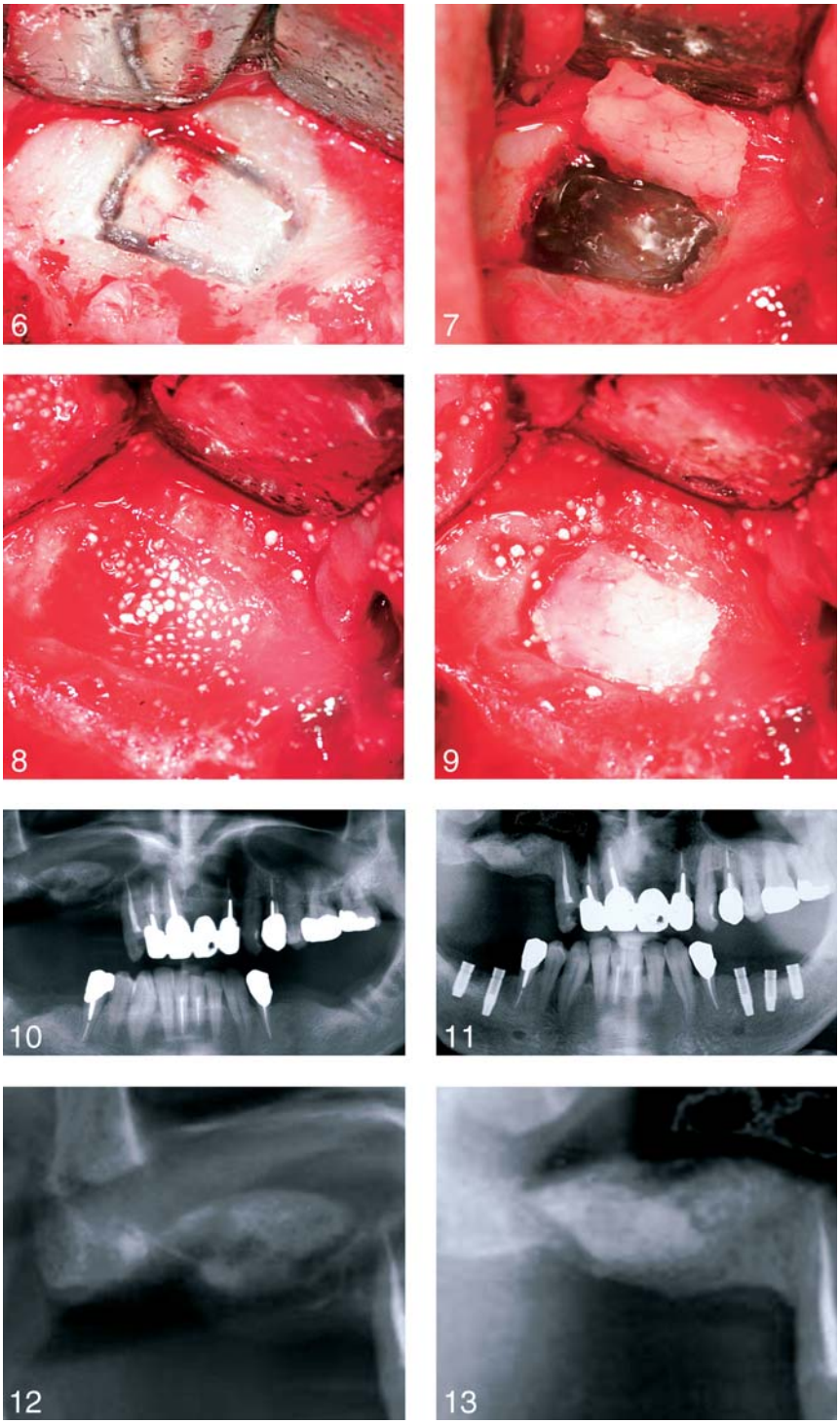

FIGURES 6–13. FIGURES 6–9. Clinical phases of the 2-step maxillary sinus augmentation with engineered porous hydroxyapatite (HA). FIGURE 10. Postoperatory orthopantomography. FIGURE 11. Radiograph 5 months after. Note the bone density obtained 5 months after the surgery. Now the placement of the implants will be possible. FIGURES 12–13. At greater magnification, note the bone density before and 5 months after the maxillary sinus elevation procedure with porous HA.

tion of osteoblasts inside the pore network.[16] This kind of architecture effectively promotes angiogenesis inside the pore system and interconnections, and blood vessels are able to carry cells and soluble signals promoting bone formation and finally bone regeneration.[17–27] All these data are confirmed by several in vitro and in vivo studies with porous HA biomaterials that have been shown to be well colonized by osteoblasts.[28–31] According to the recent acquisitions on bone physiology,[32] and in particular on bone reparation and formation processes, porous HA has been chemically, physically, and structurally modified with the aim to reproduce and to ''mime'' all the characteristics of bone tissue. This produces a better interaction between HA and bone processes. In fact, porous HA materials show the suitable characteristics to bond directly to bone tissue and can integrate with it, but they can also enhance new bone formation by acting as promoters and inductors for fundamental specific physiological events. Therefore, they assume the name of ''intelligent'' materials or ''biomimetic biomaterials.''[33–35] By modifying some compositional parameters (eg, Ca/P ratio, structure, surface, porosity, chemistry), we can obtain specific materials with peculiar customized activity such as resorption, mechanical resistance, porosity, and granulometry. The clinical use of macro- and microporous biomaterials has proven to be a safe and reliable procedure, as confirmed by several clinical trials and studies in humans, particularly in cases of reconstruction of severe bone defects.[36–41] The aim of this study was to evaluate the clinical behavior and the histological and ultrastructural aspects of porous

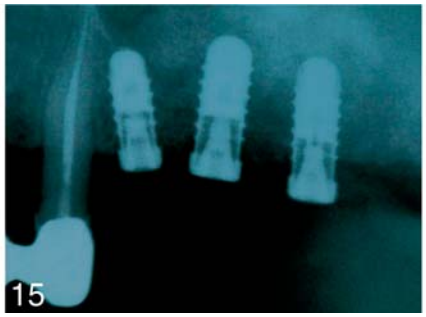

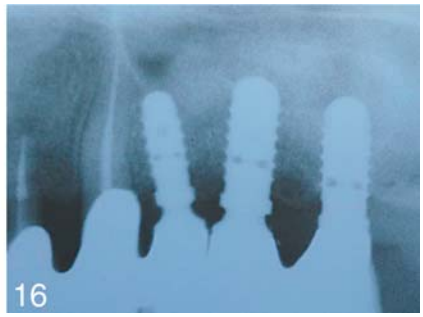

FIGURES 14–16. FIGURE 14. Another case of maxillary sinus augmentation. In this case the sinus floor elevation is performed at the time of implant placement (1-step procedure); radiograph is performed at the time of surgery (FIGURE 15) and 3 years after (FIGURE 16). All implants are in function.

HA in maxillary sinus augmentation procedures.

MATERIALS AND METHODS

Material characteristics

Engipore (Finceramica SRL, Faenza, Italy), a novel porous HA material with specific characteristics (Figure 1), was evaluated in this study. A complete physicochemical and morphological characterization of Engipore was performed through the analysis of design and distribution of macro- and microporosity and pore dimensions. Porosity was studied with an image analyzer (Q500MW, Qphase Application, Leica Imaging System Ltd, Wetzlar, Germany) in conformity with ASTM E562, morphology was analyzed by scanning electron microscopy (SEM) (Leica, Cambridge, UK), and mineralogical and chemical characterization was performed by X-ray diffractometry (CuKa radiation, Rigaku Miniflex, Kent, UK) and by inductively coupled plasma spectroscopy (Spectroflame Modula, Spectro, with Ultrasonic Nebulizer Cetac U-6000 AT, Omaha, Neb) (Figures 2 through 5). Engipore blocks were mechanically characterized, too, so that compressive strength and flexibility values were determined. The results of all these studies showed that Engipore block powder is a pure HA with a stoichiometrical ratio of 1:67, whereas Engipore granule powder reveals a nonstoichiometrical ratio (Ca + Mg/P = 1:71). Porosity is about 90% (±3%), and pore distribution is bimodal with pore diameter between 100 and 200 mm (32%) and 200 and 500 mm (40%). Compressive strength is 8.2 MPa (±0.36) and flexibility is 1.35 MPa (±0.36). Morphological analysis by SEM revealed homogenous distribution of macro- and microporosity, and HA crystallinity is very similar to bone, as shown by X-ray diffractometry.

Patient selection

Twenty-four patients (19 men, 5 women) in good general physical and mental health and with partially or completely edentulous maxillae were selected for this study. Patient age ranged from 30 to 63 years, with an average of 53.4 years. Patients presented good oral health and no active periodontal disease, and only 4 were smokers. A total of 57 screw-shaped titanium dental implants (Leader Implant System, Milan, Italy) were placed. All patients needed sinus floor elevation (5 of them bilaterally) because overall lateral alveolar bone height was less than 8 mm (vertical bone height). Forty-six implants were placed by a 1-stage procedure at the time of reconstructive surgery. Eleven implants required a 2-stage procedure (first stage: grafting; second stage: placement of the implants) because less than 4 mm of bone height at the most inferior point of the maxillary sinus was conserved, and the residual original bone of the alveolar crest was not adequate to obtain primary implant stability. The Ethic Committee of our university approved the protocol, and all patients signed a written informed-consent form.

Surgical procedure

Patients were given antibiotic prophylaxis before sinus floor augmentation surgery. The surgical procedure was carried out according to Tatum.[42] After a horizontal crestal incision and 2 vertical incisions in the buccal mucosa, a pedicled mucoperiosteal flap was raised to expose the lateral wall of the maxillary sinus. A bone window approximately 1 × 1 cm was outlined with a round bur, and the final perforation of bone was performed with a diamond bur at 2000 rpm under constant saline irrigation. Care was taken not to penetrate the schneiderian membrane. The sinus mucosa was separated from the bony surface of the sinus floor

with an elevator. The bony window fragment was moved mesially. In all cases of 2-stage procedure (n = 11), after sinus floor elevation the space created between the maxillary alveolar process and the new sinus floor was filled with Engipore blocks that were shaped and modeled by the surgeon. In fact, Engipore blocks can be easily and rapidly adapted to the defect size at the time of surgery. Engipore granules were used to fill the small gaps between porous material blocks and residual bone crest. The granules were mixed with tetracycline powder to obtain a local antibiotic effect, and this mixture was watered by physiological solution so that the composition could be more easily handled to fit in the gaps. Implant insertion was performed simultaneously (1-stage procedure, n = 46) only if a minimum bone height of 4 mm was conserved in order to guarantee primary implant stability. In the simultaneous procedure, Engipore blocks were packed to the medial aspect of cavity, then implants were inserted and primary stability was evaluated. Finally, Engipore granules mixed with tetracycline powder (as previously described) were packed and condensed in the residual space to fill the defect completely. In all cases (1- and 2-stage procedures) no membrane was used. Complete wound closure was performed with nonresorbable sutures (SKD sutures, TecnoDenta, Milan, Italy) (Figures 6 through 16). Analgesics (nimesulid) were administered, and an irrigant (0.2% chlorhexidine) was prescribed for oral hygiene. Suture removal was performed 10 days after the surgical procedure. In the 2-stage procedures, the grafted sinuses were allowed to heal for 6 months before implant placement.

Specimen retrieval

Six months after sinus floor elevation, at the time of dental implant placement, biopsies were carried out under local anesthesia. Biopsies were taken with a 2.5-mm-diameter trephine burr (Straumann, Waldenburg, Switzerland) under copious irrigation with sterile saline. Eleven biopsies were taken at the sites where dental implants would be placed. These bone cores were cut in half and were processed for light and transmission electron microscopy.

Specimen processing

Light Microscopy

The specimens were immediately fixed in 10% buffered formalin and processed to obtain thin ground sections with the Precise 1 Automated System (Assing, Rome, Italy). The specimens were dehydrated in an ascending series of alcohol rinses and embedded in a glycolmethacrylate resin (Technovit 7200 VLC, Kulzer, Wehrheim, Germany). After polymerization, the specimens were sectioned along their longitudinal axes with a high-precision diamond disc at about 150 μm and were ground down to about 30 μm with a specially designed grinding machine. The slides were stained with acid fuchsin and toluidine blue. The slides were observed in normal transmitted light under a Leitz Laborlux microscope (Wetzlar, Germany). Histomorphometrical analysis was performed with a computer AMD 1800 Mz with a digital video color card RGB (Matrix Vision, GmbH, Oppenweiler, Germany); a color camera 3CCD, JVC KY-F55B (GT Vision Ltd, Suffolk, UK) and Image-Pro Plus 4.5 software (Media Cybernetics Inc, Immagini Computer SNC, Milan, Italy) to investigate the percentage of biomaterial, bone, and bone marrow spaces.

Transmission Electron Microscopy

The retrieved specimens were washed in a saline solution and quickly immersed in 2.5% glutaraldehyde and 2.5% formaldehyde (freshly prepared from paraformaldehyde) buffered at pH 7.2 with 0.1 M sodium phosphate for 4 hours at room temperature and were left overnight at 4°C. After washing for 1 hour in the buffer alone, some specimens were left mineralized for light microscopy evaluation. The remaining specimens were decalcified with 4.13% EDTA (Sigma, Deisenhofen, Germany). These specimens were postfixed in 1% cacodylate buffered osmium tetroxide for 1 hour, dehydrated in graded concentrations of ethanol, and embedded in LR White resin (Berkshire, London). Toluidine blue–stained 1-μm-thick sections were obtained and examined under a light microscope. Next, selected regions were trimmed for ultrathin sectioning. Ultrathin sections were collected on copper grids, stained with lead citrate and uranyl acetate, and examined in a Jeol 1010 transmission electron microscope (Pieve Emanuele, Italy) operated at 60 kV.

RESULTS

Clinical results

A total of 57 implants in lengths of 10 to 14 mm were placed, 46 simultaneously and 11 in a staged procedure (with an average healing time of 6 months after sinus grafting). Loading of implants was performed after a mean time of 4.4 months after insertion, consisting of 4.0 months after a staged procedure or 5.2 months after a simultaneous procedure. To date, a mean 3 years after

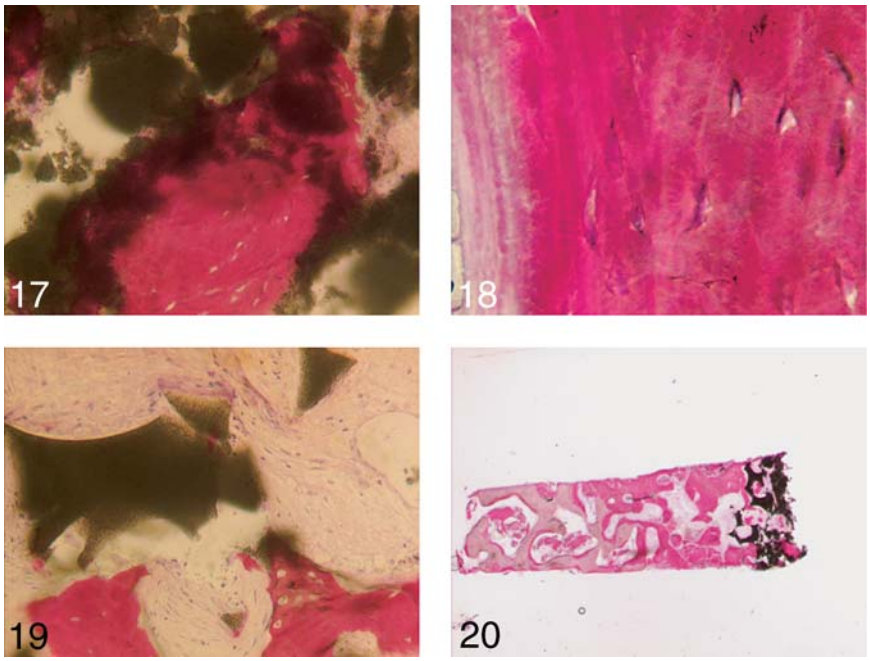

FIGURES 17–20. FIGURE 17. Newly formed bone was in close contact with the biomaterial particles. It is possible to observe a more porous appearance of the particles in a phase of degradation (acid fuchsin and toluidine blue, original magnification ×100). FIGURE 18. At higher magnification, at the interface, there was osteoid matrix, lightly stained by acid fuchsin and newly formed bone, strongly stained by acid fuchsin. Moreover, it is possible to observe small osteocyte lacunae (acid fuchsin and toluidine blue, original magnification ×200). FIGURE 19. Osteoblasts actively secreting osseous tissue and osteoclasts actively resorbing biomaterial particles are present (acid fuchsin and toluidine blue, original magnification ×50). FIGURE 20. At higher magnification, in the coronal portion, it was possible to observe the presence of mature trabecular bone, with peripheral remodeling processes; in the midportion of the core, there was newly formed bone tissue with a higher staining for acid fuchsin and many areas of active osteoblasts that were deposing osteoid matrix; and in the apical portion, it was possible to observe the presence of small residues of the biomaterial, and some of them appeared to undergo resorption processes (acid fuchsin and toluidine blue, original magnification ×6).

implantation, all implants are clinically in function, and no surgical or prosthetic complications have occurred. No clinical signs of sinus pathology were observed, and no patients showed any sign of maxillary sinusitis. Clinical and radiological follow-up examinations were performed immediately after the surgery, 3 months later, and every 6 months thereafter for the next 2 years. The clinical parameters evaluated were bleeding on probing and probing depth.[43] Bleeding on probing was measured on each implant with a calibrated periodontal probe, and no bleeding was noted, whereas the mean value of probing depth (the depth of peri-implant probe penetration in millimeters taken at the mesial, distal, vestibular, and palatal sites) was 2.84 mm at a 3-year follow-up, showing a very good stability of the peri-implant–integrated tissues. Radiographical analysis was performed by single-tooth X-rays and panoramic radiographs. Six months after surgery, the radiograph analysis confirmed a postgrafting opacity of the maxillary sinus floor in all patients. Vertical peri-implant bone levels were studied, too, at different times at the mesial and distal aspect of each implant. The aim was to calculate the vertical bone levels or the distance in millimeters from the implant shoulder to the first crestal bone to implant contact and the vertical bone loss 3 years after functional loading. The dimensions known for each implant were used as reference lengths so that the magnification could be compensated. We discovered that the mean distance between the implant shoulder and the first visible bone contact was 2.10 mm after 3 years, with a mean marginal bone loss during the first year of function of only 0.26 mm. All these data reveal a low tendency to marginal bone resorption and a good stability of peri-implant bone tissue.

Light microscopy

In many fields, newly formed bone was in close contact with the biomaterial particles (Figure 17). No gaps were present at the bone-biomaterial interface. In some areas there was osteoid matrix at the interface lightly stained by acid fuchsin. The newly formed bone was strongly stained by acid fuchsin and contained small osteocyte lacunae (Figure 18). The newly formed bone presented a trabecular appearance with no osteonic structures. In the regions where bone was not in contact with the biomaterial particles, areas of resorption were visible on the particle surfaces. Only a few mono- or multinucleated cells were present in these areas (Figure 19). No acute inflammatory infiltrate was present. In many fields it was possible to observe that most of the particles were united by the newly formed bone. In the coronal portion it was possible to observe the presence of mature trabecular bone, whereas in the midportion of the core there was

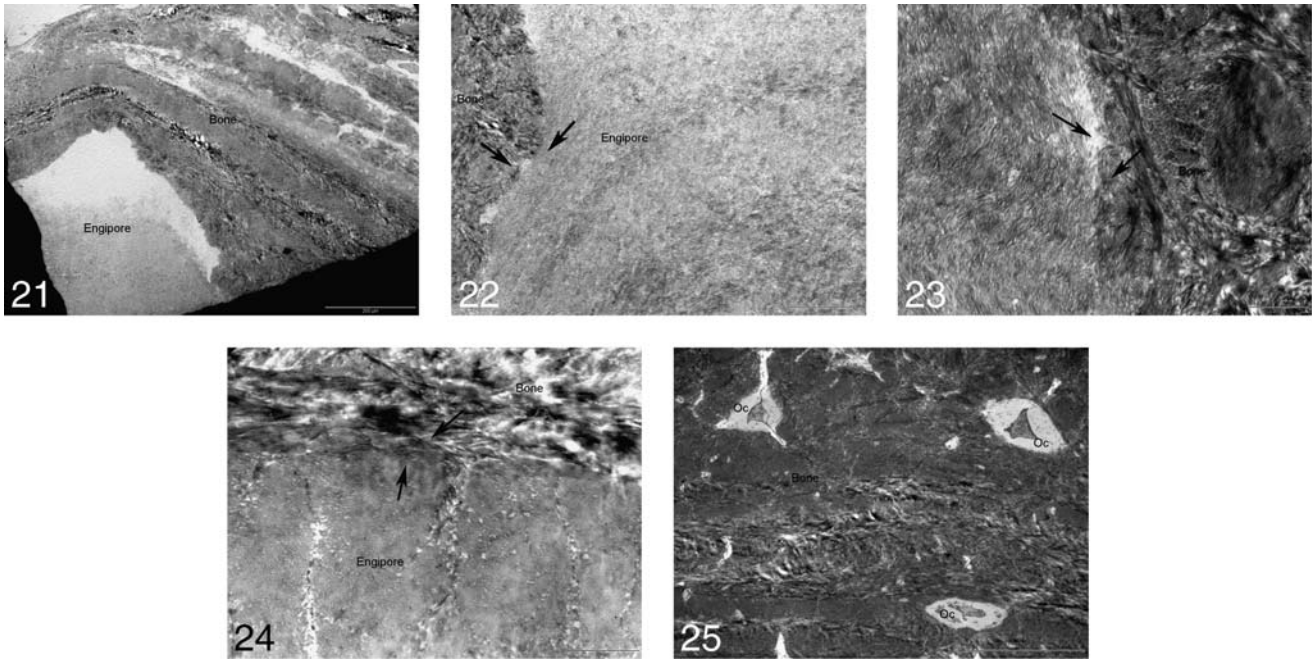

FIGURES 21–25. FIGURE 21. Transmission electron micrograph. At this original magnification (×2000) it is possible to visualize the particle of Engipore surrounded by mature bone. The upper portion of the particle shows a partial detachment from the bone because of the ultrathin sectioning procedure. The mature bone is composed multiple lamellae that appear well organized. Bar = 200 μm. FIGURE 22. Transmission electron micrograph. At this original magnification (×5000) there is no gap at the interface between Engipore particle and bone. The internal structure of the biomaterial appears amorphous and is in close contact with the bone (arrows) that showed features of compact osseous tissue. Bar = 50 μm. FIGURE 23. Transmission electron micrograph at original magnification (×20 000). In some cases the Engipore particles are surrounded by a layer of a not-yet-mineralized osteoid seam with randomly distributed collagen fibrils. This tissue is in close contact (arrows) with the mineralized tissue (bone) that is mainly compact and well organized. Bar = 20 μm. FIGURE 24. Transmission electron micrograph at original magnification (×20 000). The Engipore particle seems to be perfectly integrated into the compact bone (arrows), which departs from the biomaterial without any space in between. Bar = 20 μm. FIGURE 25. Transmission electron micrograph at original magnification (×2000). The bone around the particles and among them is mainly compact, organized in multiple lamellae, and colonized by numerous osteocytes (Oc) that lay down in their osteocytic lacunae and show few cytoplasmatic processes. Bar = 200 μm.

newly formed bone tissue with a higher staining for acid fuchsin. In this portion it was possible to observe the presence of small residues of the biomaterial. A higher quantity of residual biomaterial was present in the apical portion (Figure 20). At higher magnification, the bone tissue was mature in the coronal portion, and remodeling processes were apparent in the peripheral portions of the bone. In the midportion of the specimen newly formed bone was present with many areas of active osteoblasts that were deposing osteoid matrix. In the apical portion some of the biomaterial particles appeared to undergo resorption processes. Newly formed bone was 38.5% ± 4.5%, whereas the residual biomaterial represented 12% ± 2.3% and the marrow spaces represented 44.6% ± 4.2%.

Transmission electron microscopy

In the majority of the cases the biomaterial particles were in close contact with the bone, which appeared compact and presented some osteocytes inside (Figure 21). The particles did not contain a cellular component and appeared amorphous, fibrillar, and not well organized.

The limit between the particle and the bone was distinguishable by a change in the electron density of the 2 structures. Indeed, the biomaterial structure appeared less electron dense than the bone surrounding it; however, it seemed to be in natural contiguity with the bone. In particular, a cementlike line was slightly visible at the bone-biomaterial interface, but there was no gap or interposed connective tissue in between (Figure 22). In some cases, bundles of collagen fibrils were present at this interface, probably indicating a continuous process of new bone formation at the interface (Figure 23). The bone surrounding the particles showed the characteristic features of a well-organized la-

mellar bone with readily visible transverse and longitudinal collagen fibers and small marrow spaces (Figure 24). There were old osteocytes with scarce cytoplasm embedded in their calcified matrices, and a few inflammatory cells such as histiocytes were sometimes present (Figure 25).

Discussion

The use of biomimetic biomaterials capable of promoting new bone formation through the mechanism of osteoinduction has marked the passage from bone regeneration to bone tissue engineering. On that account, it is very important to differentiate an osteoinductive biomaterial from an osteoconductive one: the former has the capacity to guide and direct the growth of bone at its interfaces and to achieve osteointegration after implantation in extraskeletal sites (orthotopically), whereas the latter promotes new bone formation by itself, even if implanted in extraskeletal sites (heterotopically). In fact, the test for osteoinductivity is the histological evidence of bone formation in heterotopic sites in animals. Ripamonti[34,35] has demonstrated that some particular highly porous HA materials are capable of inducing bone differentiation in intramuscular sites of nonhuman primates (eg, Chacma baboons [*Papio ursinus*]). Many other authors have successfully shown the phenomenon of ectopic osteoinduction by using calcium-phosphate–based materials in different animal models.[17–27] All these studies have shown that porous HA can act as a solid-state matrix (carrier substratum) for the adsorption, concentration, and controlled release of circulating or locally produced bone-morphogenic/osteogenic proteins (BMPs/Ops) capable of inducing new bone formation.[44–48] Bone-morphogenic proteins show high affinity for HA. In fact, chromatographic adsorption of naturally derived mammalian BMPs onto gels of HA has been demonstrated to be a fundamental step in their purification.[44] Histological and immunohistochemical studies have demonstrated that localization of BMP family members at the interface between mesenchymal tissue generated within the concavities and the HA substratum represents the first step before bone regeneration occurs. A required critical concentration of BMPs is necessary for the initiation of bone formation. First, circulating and endogenously produced BMPs/Ops are bound to the substratum, and then they induce new bone formation at higher concentrations. On the other hand, the geometry of the HA substratum plays a critical role because it can profoundly regulate the expression of the osteogenic phenotype, as previously demonstrated.[49] Novel porous HA is designed with specific geometric characteristics because it is well known that new bone formation starts in concavities rather than on plane or convex surfaces.[46] Concavities are the ideal structural and biological microenvironment for the promotion of new bone formation, as they affect cellular morphology, cellular shape, and finally cellular function.[50–54] Nanci et al[53] have demonstrated that porous HA can adsorb not only BMPs/Ops but also specific proteins from the extracellular matrix (osteopontin, bone sialoproteins) onto its surface within the pore network. These proteins play a fundamental role in the regulation of cellular adhesion and bone matrix mineralization. The porous architecture of the HA substratum, with its macropore network and its micropore interconnections, induces rapid vascular and mesenchymal invasion and provides a specific cell flow. These cells can attach, proliferate, and finally differentiate into functional osteoblasts.

Conclusions

The results of our study show that porous HA can be a suitable synthetic material for bone regeneration in maxillary sinus augmentation procedures. A high quantity (about 40%) of newly formed bone was present. Bone was closely apposed to the biomaterial particles as shown in light microscopy and transmission electron microscopy. Moreover, no signs of inflammatory cell infiltrate or foreign body reaction were present. Also, most of the biomaterial was resorbed, and only a small quantity (slightly more than 10%) was still present.

The important advancements in the fascinating field of tissue engineering will produce new biomimetic biomaterials (highly porous HA substrata) capable of inducing bone formation, acting as delivery systems for both growth factors (BMPs/Ops and many other soluble signals) and stem cells thanks to their chemical characteristics and, most of all, their peculiar geometric structure. These novel substrata will promote bone formation by themselves.

Acknowledgments

This work was partially supported by the National Research Council, Rome, Italy; by the Ministry of Education, University and Research, Rome, Italy; and by the Research Association for Dentistry and Dermatology, Chieti, Italy.

References

1. Raghoebar GM, Louwerse C, Kalk WW, Vissink A. Morbidity of chin bone

harvesting. *Clin Oral Implants Res.* 2001;12:503–507.

2. Wykrota LL, Wykrota FHL. Long term bone regeneration in large human defects using calcium-phosphate particulate. In: Davies JE, ed. *Bone Engineering.* Toronto, Canada: EM Squared Inc; 2000:515–547.

3. Buck BE, Malinin TI, Brown MD. Bone transplantation and human immunodeficiency virus (HIV): an estimate of risk of acquired immunodeficiency (AIDS). *Clin Orthop.* 1989;240:129–136.

4. Centers for Disease Control and Prevention. Transmission of HIV through bone transplantation: case report and public health recommendations. *MMWR Morb Mortal Wkly Rep.* 1998;37:597.

5. Buck BE, Resnick L, Shah SM, Malinin TI. Human immunodeficiency virus cultured from bone: implications for transplantation. *Clin Orthop.* 1990; 251:249–253.

6. Jarcho M. Calcium phosphate ceramics as hard tissue prosthetics. *Clin Orthop.* 1981;157:259–278.

7. LeGeros RZ. Calcium phosphate materials in restorative dentistry: a review. *Adv Dent Res.* 1988;2:164–180.

8. Hollinger JO, Brekke J, Gruskin E, Lee D. Role of bone substitutes. *Clin Orthop.* 1996;324:55–65.

9. Clokie CML, Coulson R, Peel SAF, Sandor GKB. Approaches to bone regeneration in oral and maxillofacial surgery. In: Davies JE, ed. *Bone Engineering.* Toronto, Canada: EM Squared Inc; 2000:558–576.

10. Mangano C, Piattelli A, Scarano A, Martinetti R. *L'idrossiapatite in Chirurgia Orale.* Milano, Italy: Utet Periodici; 1998.

11. Mangano C, Ripamonti U, Mangano F, Montini S, Martinetti R. Ingegneria tessutale, induzione ossea e biomateriali biomimetici. *Implantologia Orale.* 2004;5:9–35.

12. De Groot K. Degradable ceramics. In: Williams DF, ed. *Biocompatibility of Implant Materials.* Vol 1. Boca Raton, Fla: CRC Press; 1981:199.

13. Tadic D, Epple M. A thorough physicochemical characterization of 14 calcium-phosphate based bone substitution materials in comparison to natural bone. *Biomaterials.* 2004;25:987–994.

14. Yuan H, Kurashina K, De Bruijn JD, et al. A preliminary study on osteoinduction of two kinds of calcium phosphate ceramics. *Biomaterials.* 1999; 20:1799–1806.

15. Mangano C, Bartolucci E. A new porous hydroxyapatite for promotion of bone regeneration in maxillary sinus augmentation: clinical and histological study in humans. *Int J Oral Maxillofac Implants.* 2003;18:20–30.

16. Ripamonti U, Crooks J, Kirkbride AN. Sintered porous hydroxyapatite with intrinsic osteoinductive activity: geometric induction of bone formation. *S Afr J Sci.* 1999;95:335–343.

17. Vagervik K. Critical sites for new bone formation. In: Habal MB, Reddi AH, eds. *Bone Grafts and Bone Substitutes.* Philadelphia, Pa: WB Saunders; 1992: 112–120.

18. Yamasaki H, Saki H. Osteogenic response to porous hydroxyapatite ceramics under the skin of dogs. *Biomaterials.* 1992;13:308–312.

19. Toth JM, Lynch KL, Hackbarth DA. Ceramic-induced osteogenesis following subcutaneous implantation of calcium phosphates. *Bioceramics.* 1993; 6:9–13.

20. Klein CPAT, De Groot K, Chen W, Li Y, Zhang X. Osseous substance formation induced in porous calcium phosphate ceramics in soft tissues. *Biomaterials.* 1994;15:31–34.

21. Yang Z, Yuan H, Tong W, Zou P, Chen W, Zhang X. Osteogenesis in extraskeletally implanted porous calcium phosphate ceramics: variability among different kinds of animals. *Biomaterials.* 1996;17:2131–2137.

22. Yang Z, Yuan H, Zou P, Tong W, Qu S, Zhang X. Osteogenic response to extraskeletally implanted synthetic porous calcium phosphate ceramics: an early stage histomorphological study in dogs. *J Mater Sci Mater Med.* 1997;8:687–701.

23. Yuan H, Yang Z, Zou P, Li Y, Zhang X. Rapid osteogenesis in porous biphasic calcium phosphate ceramics implanted in domestic pigs. *Biomedical Engineering—Application, Basis, and Communications.* 1997;9:268–273.

24. Yuan H, Li Y, Yang Z, Feng J, Zhang X. An investigation on the osteoinduction of synthetic porous phase—pure hydroxyapatite ceramic. *Biomedical Engineering—Application, Basis, and Communications.* 1997;9:274–278.

25. Yuan H, Li Y, Yang Z, Feng J, Zhang X. Calcium phosphate ceramic induced osteogenesis in rabbits. In: Zhang X, Ikada Y, eds. *Biomedical Material Research in the Far East (III).* Kyoto, Japan: Kobunshi Kankokai; 1997:228–229.

26. Yuan H, Li Y, Yang Z, Zhang X. Osteoinduction of pure beta-TCP ceramic in dogs. In: Zhang X, Ikada Y, eds. *Biomedical Material Research in the Far East (III).* Kyoto, Japan: Kobunshi Kankokai; 1997:188–189.

27. Yuan H, Li Y, Kurashina K, Zhang X. Host tissue responses on calcium phosphate cement. In: Zhang X, Ikada Y, eds. *Biomedical Material Research in the Far East (III).* Kyoto, Japan: Kobunshi Kankokai; 1997:116–117.

28. Rout PGJ, Tarrant SF, Frame JW, Davies JE. Interactions between primary bone cell cultures and biomaterials part 3. A comparison of dense and macroporous hydroxyapatite. In: Pizzoferrato A, Ravaglioli PG, Lee AJC, eds. *Biomaterials and Clinical Applications.* Amsterdam, The Netherlands: Elsevier; 1987: 591–596.

29. Petite H, Kacem K, Triffitt JT. Adhesion, growth and differentiation of human bone marrow stromal cells on non-porous calcium carbonate and plastic substrata: effects of dexamethasone and 1,25 dihydroxyvitamin D3. *J Mater Sci Mater Med.* 1996;7:665–671.

30. Davies JE, Baldan N. Scanning electron microscopy of the bone-bioactive implant interface. *J Biomed Mater Res.* 1997;36:429–440.

31. Holy CE, Shoichet MS, Davies JE. Bone marrow cell colonization of, and extracellular matrix expression on biodegradable polymers. *Cells Mater.* 1997;7:223–234.

32. Davies JE, Hosseini MM. Histodynamics of endosseous wound healing. In: Davies JE, ed. *Bone Engineering.* Toronto, Canada: EM Squared Inc; 2000; 1:1–14.

33. Healy KE, Harbers GM, Barber TA, Sumner DR. Osteoblast interactions with engineered surfaces. In: Davies JE, ed. *Bone Engineering.* Toronto, Canada: EM Squared Inc; 2000;24:268–281.

34. Ripamonti U. Osteoinduction in porous hydroxyapatite implanted in heterotopic sites of different animal models. *Biomaterials.* 1996;17:31–35.

35. Ripamonti U. The morphogenesis of bone in replicas of porous hydroxyapatite obtained from conversion of calcium carbonate exoskeletons of coral. *J Bone Joint Surg Am.* 1991;73A:692–703.

36. Kruger E. Reconstruction of bone and soft tissue in extensive facial defects. *J Oral Maxillofac Surg.* 1982;40:714–720.

37. Kent N, Quinn JH, Zide MF, Finger IM, Jarcho M, Rothstein SS. Correction of alveolar ring deficiencies with non-resorbable hydroxyapatite. *J Am Dent Assoc.* 1982;105:993–1001.

38. Kent JN, Quinn JH, Zide MF, Guerra LR, Boyne PJ. Alveolar ridge augmentation using non resorbable hydroxyapatite with or without autogenous cancellous bone. *J Oral Maxillofac Surg.* 1983;41:629–642.

39. Osnish H. Clinical results versus experimental data in orthopaedic application of bioceramic. In: Ducheyne P, Christiansen D, eds. *Bioceramics*. Vol 6. Oxford, England: Butterworth-Heinemann; 1993.

40. Nakamura S, Kitawto I. Efficiency of hydroxyapatite tricalcium phosphate composite (HAP-TCP) for bone defect tibial fracture: comparison between HAP-TCP and autogenous iliac bone. In: Andersson OH, Yli-Urpo A, eds. *Bioceramics*. Vol 7. Cambridge, England: Butterworth-Heinemann; 1994: 435–440.

41. Hori M, Munemiya M, Takahashi S. Efficiency of hydroxyapatite tricalcium phosphate composite (HAP-TCP) for bone defect tibial fracture: comparison between HAP-TCP and autogenous iliac bone. In: Andersson OH, Yli-Urpo A, eds. *Bioceramics*. Vol 7. Cambridge, England: Butterworth-Heinemann; 1994:435–440.

42. Tatum H. Maxillary and sinus implant reconstructions. *Dent Clin North Am.* 1986;30:207–229.

43. Fiorellini JP, Weber HP. Clinical trials on the prognosis of dental implants. *Periodontol 2000.* 1994;4:98–108.

44. Ripamonti U, Crooks J, Kirkbride AN. Sintered porous hydroxyapatite with intrinsic osteoinductive activity: geometric induction of bone formation. *S Afr J Sci.* 1999;95:335–343.

45. Ripamonti U, Van den Heever B, van Wyk J. Expression of the osteogenic phenotype in porous hydroxyapatite implanted extraskeletally in baboons. *Matrix.* 1993;13:491–502.

46. van Eeden S, Ripamonti U. Bone differentiation in porous hydroxyapatite is regulated by the geometry of the substratum: implications for reconstructive craniofacial surgery. *Plast Reconstr Surg.* 1994;93:959–966.

47. Magan A, Ripamonti U. Geometry of porous hydroxyapatite implants influences osteogenesis in baboons. *J Craniofac Surg.* 1996;7:71–78.

48. Ripamonti U. Inductive bone matrix and porous hydroxyapatite composites in rodents and in non-human primates. In: Yamamuro T, Wilson-Hench J, Hench L, eds. *Handbook of Bioactive Ceramics.* Boca Raton, Fla: CRC Press; 1990:245–253.

49. Singhvi R, Stephanopolous G, Wang D. Review: effects of substratum morphology on cell physiology. *Biotech Bioeng.* 1993;43:764–771.

50. Folkman J, Greenspan HP. Influence of geometry on control of cell growth. *Biochim Biophys Acta.* 1975;417:211–236.

51. Gospodarowicz D, Greenburg G, Birdwell CR. Determination of cellular shape by the extracellular matrix and its correlation with the control of cellular growth. *Cancer Res.* 1978;38:4155–4171.

52. Bissell MJ, Barcellos-Hoff MH. The influence of extracellular matrix on gene expression: is structure the message? *J Cell Sci Suppl.* 1987;8:327–343.

53. Nanci A, Zazal S, Fortin M, Mangano C, Goldberg HA. Incorporation of circulating bone-matrix proteins by implanted hydroxyapatite and at bone surfaces: implications for cement-line formation and structuring of biomaterials. In: Davies JE, ed. *Bone Engineering.* Toronto, Canada: EM Squared Inc; 2000:305–311.

54. De Bruijn JD, Yuan H, Dekker R, Layrolle P, de Groot K, van Blitterswijk CA. Osteoinductive biomimetic calcium-phosphate coatings and their potential use as tissue-engineering scaffolds. In: Davies JE, ed. *Bone Engineering*. Toronto, Canada: EM Squared Inc; 2000:421–430.